

Magnitude and Wrap-Phase OFDM for MIMO Visible Light Communication Systems

Mohamed Al-Nahhal¹, Student Member, IEEE, Ertugrul Basar², Senior Member, IEEE,
and Murat Uysal², Fellow, IEEE

Abstract—Generalized light emitting diode (LED) index modulation (GLIM) has been proposed as an effective multiple-input multiple-output (MIMO) orthogonal frequency division multiplexing (OFDM) scheme for visible light communications (VLC) systems. In this letter, we propose a magnitude and wrap-phase OFDM (MW-OFDM) scheme for MIMO VLC systems. The proposed MW-OFDM system relies on the conversion of complex signals into polar form with the magnitudes and wrap-phases to decrease the restriction on the number of LEDs compared to the conventional GLIM-OFDM. Furthermore, maximum likelihood and best linear unbiased estimators of the proposed scheme are derived. The proposed MW-OFDM scheme improves the average bit error rate and provides a significant reduction in the decoding complexity, compared to the GLIM-OFDM. Moreover, a half number of LEDs are required for the proposed scheme to deliver the same spectral efficiency in a comparison with the GLIM-OFDM. Numerical results are presented over MIMO VLC channels to elaborate the superiority of our proposed scheme.

Index Terms—Visible light communications, multiple-input multiple-output, orthogonal frequency division multiplexing, maximum likelihood estimator, decoding complexity.

I. INTRODUCTION

VISIBLE light communications (VLC) is a new wireless technology which has been proposed as a complementary or alternative solution to radio frequency-based counterparts. VLC has distinct advantages such as operation in unlicensed spectrum, high energy efficiency, and high data transmission rates [1]. The VLC systems utilize light emitting diodes (LEDs) at the transmitter side to deliver the information, whereas the photodetectors (PDs) are used at the receiver side. Thus, LEDs can be used for wireless transmission purposes in addition to their basic purpose of illumination.

VLC systems build upon intensity modulation and direct detection due to LEDs' characteristics [2]. Therefore, initial studies for the VLC systems are focused on simple modulation techniques, such as on-off keying and pulse modulation techniques, to deal with the limitations of LEDs [3]. However, the selectivity of the VLC channels significantly deteriorates the VLC system performance due to severe inter-symbol

interference (ISI). This motivates the use of optical orthogonal frequency division multiplexing (OFDM) techniques, such as DC-biased optical OFDM (DCO-OFDM), asymmetrically clipped optical OFDM (ACO-OFDM) and unipolar OFDM (U-OFDM), to overcome the ISI [2, Ch. 12], [4]. In DCO-OFDM, ACO-OFDM and U-OFDM, the Hermitian symmetry of the fast Fourier transformation (FFT) is required to obtain a bipolar signal. To solve the bipolarity problem, the DCO-OFDM utilizes the DC bias subsequent to the inverse FFT (IFFT) operation. Whereas the ACO-OFDM eliminates the DC bias at the expense of sacrificing half of the spectral efficiency, compared to DCO-OFDM. In U-OFDM, the positive and negative samples of the bipolar signal, resulted from the IFFT operation, are transmitted separately into two different OFDM frames [5]. As a result, the U-OFDM achieves a better bit error rate (BER) at the expense of sacrificing half of the spectral efficiency in a comparison with the DCO-OFDM. In [6]–[8], the polar OFDM (P-OFDM) technique has been proposed for single-input single-output VLC systems, where each complex sample resulted from IFFT is converted into magnitude and wrap-phase to be transmitted sequentially, which limits the spectral efficiency. The P-OFDM achieves twice of spectral efficiency compared to the ACO-OFDM, and improves the energy-efficient of the VLC systems. The concept of using the magnitude and phase transmission through the multiple LEDs has been studied for single-carrier VLC systems in [9]–[11].

Recently, generalized LED index modulation (GLIM) has been proposed as a promising scheme for multiple-input multiple-output (MIMO) OFDM VLC systems [12]–[14]. In the GLIM-OFDM scheme, the real and imaginary parts of complex samples are transmitted from separate two groups of LEDs and only one LED is active from each group. In other words, the GLIM-OFDM utilizes the index modulation concept for the active LEDs to transmit the real and imaginary parts of complex OFDM signals, where the indices of active LEDs indicate the sign of both parts. At the receiver side, the GLIM-OFDM utilizes a conditional maximum a posterior probability (MAP) estimator to estimate those real and imaginary parts. The GLIM-OFDM scheme achieves a higher spectral efficiency and better BER performance than the existing MIMO OFDM schemes since it does not require a Hermitian symmetry or DC bias. However, the GLIM-OFDM scheme suffers from a restriction on the number of LEDs, where it requires four LEDs to transmit one sample. Moreover, the signs of the real and imaginary values are estimated by considering all possible active LED pair scenarios which leads to an increase in the complexity of the VLC systems.

In this letter, we propose the so-called magnitude and wrap-phase OFDM (MW-OFDM) scheme for MIMO VLC systems.

Manuscript received March 8, 2021; accepted March 22, 2021. Date of publication March 31, 2021; date of current version July 10, 2021. This work was supported by the Turkish Scientific and Research Council under Grant 215E311. The associate editor coordinating the review of this letter and approving it for publication was C. Gong. (Corresponding author: Mohamed Al-Nahhal.)

Mohamed Al-Nahhal and Murat Uysal are with the Department of Electrical and Electronics Engineering, Özyeğin University, 34794 İstanbul, Turkey (e-mail: mohamed.al-nahhal@ozu.edu.tr; murat.uysal@ozyegin.edu.tr).

Ertugrul Basar is with the CoreLab, Department of Electrical and Electronics Engineering, Koç University, 34450 İstanbul, Turkey (e-mail: ebasar@ku.edu.tr).

Digital Object Identifier 10.1109/LCOMM.2021.3070272

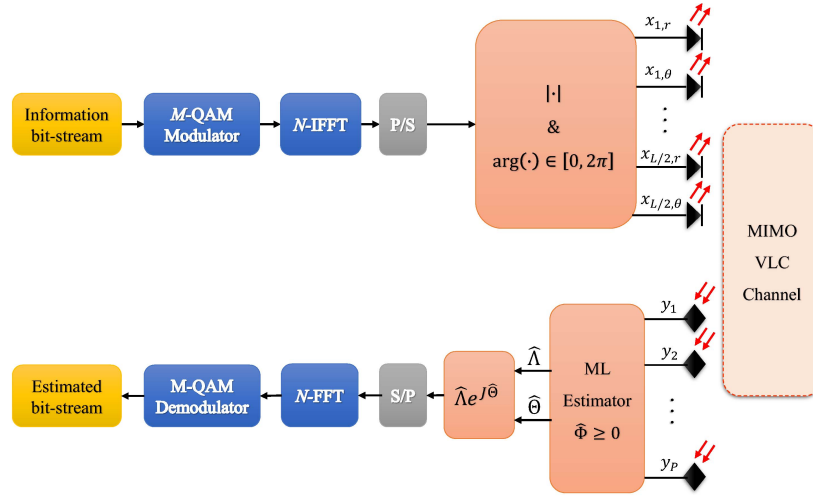


Fig. 1. Block diagram of the proposed MW-OFDM for MIMO VLC system.

We derive the maximum likelihood estimator (MLE) and the best linear unbiased estimator (BLUE) for the proposed scheme. The proposed MW-OFDM decreases the restriction on the number of LEDs and achieves better BER performance in comparison to GLIM-OFDM. This is made possible by exploiting the conversion of a complex sample into its polar form with a magnitude and a wrap-phase. As a result, the proposed MW-OFDM requires a half number of LEDs to obtain the same spectral efficiency as well as decreases the decoding complexity, compared to the GLIM-OFDM.

The rest of the letter is organized as follows: Section II presents the system model for the proposed MW-OFDM scheme. In Section III, we derive the MLE and the BLUE, and present the decoding complexity analysis for the proposed scheme. Section IV presents numerical results to evaluate and demonstrate the superiority of our proposed scheme compared to the existing schemes in the literature. Finally, concluding remarks are provided in Section V.

II. MW-OFDM SYSTEM MODEL

The block diagram of the proposed MW-OFDM scheme for a $P \times L$ MIMO VLC system is presented in Fig. 1, where P and L are the number of PDs at the receiver and LEDs at the transmitter, respectively. In the proposed MW-OFDM scheme, $N \log_2(M)$ information bit-stream is modulated using M -ary quadrature amplitude modulation (M -QAM), where N represents the number of the OFDM subcarriers and M is the modulation size. Subsequently, the modulated symbol is directly processed by the IFFT operation without using the Hermitian symmetry. After parallel-to-serial (P/S) operation, each complex OFDM sample resulting from IFFT, i.e., x_k , $k = 0, \dots, N-1$, is converted into polar form with a magnitude of $x_{k,r} = |x_k|$, and a wrap-phase of $x_{k,\theta} = \arg(x_k) \in [0, 2\pi]$. Then, the resultant magnitude and wrap-phase of each OFDM sample are transmitted simultaneously through LEDs.

The received signal $\mathbf{y} = [y_1, \dots, y_P]^T \in \mathbb{R}^{P \times 1}$ over $P \times L$ MIMO VLC channel is given by

$$\mathbf{y} = \mathbf{H}\mathbf{x} + \mathbf{w}, \quad (1)$$

where $\mathbf{H} = [\mathbf{h}_1, \dots, \mathbf{h}_L] \in \mathbb{R}^{P \times L}$ is the MIMO VLC channel matrix and \mathbf{h}_l is the l -th column of \mathbf{H} , $l = 1, \dots, L$.

The elements of \mathbf{H} are given by $h_{p,l}$ which represents the channel gain of the VLC wireless link between p -th PD and l -th LED, where $l = 1, \dots, L$ and $p = 1, \dots, P$. Here, $\mathbf{x} = [x_{1,r}, x_{1,\theta}, \dots, x_{L/2,r}, x_{L/2,\theta}]^T \in \mathbb{R}^{L \times 1}$ is the transmitted vector with magnitudes of $x_{i,r}$ and wrap-phases of $x_{i,\theta}$ for the OFDM samples for $i = 1, \dots, L/2$, and $[\cdot]^T$ denotes the transpose operation. In (1), $\mathbf{w} \in \mathbb{R}^{P \times 1}$ represents the vector of real-valued additive white Gaussian noise samples and each element has zero-mean and variance of σ_w^2 . Thus, (1) becomes

$$\begin{aligned} \mathbf{y} &= \mathbf{h}_1 x_{1,r} + \mathbf{h}_2 x_{1,\theta} + \dots + \mathbf{h}_{L-1} x_{L/2,r} + \mathbf{h}_L x_{L/2,\theta} + \mathbf{w} \\ &= \sum_{i=1}^{L/2} (\mathbf{h}_{2i-1} x_{i,r} + \mathbf{h}_{2i} x_{i,\theta}) + \mathbf{w}. \end{aligned} \quad (2)$$

As an example, assume that the k -th complex OFDM sample is $x_k = -1.5 + j2$ for $L = 2$. In the proposed MW-OFDM scheme, x_k is converted into a polar form with a magnitude of $x_{k,r} = 2.5$ and a wrap-phase of $x_{k,\theta} = 2.2143$ rad. Therefore, the transmitted vector takes the form of $\mathbf{x} = [2.5 \ 2.2143]^T$. On the other hand, the transmitted vector for GLIM-OFDM is $\mathbf{x} = [0 \ 1.5 \ 2 \ 0]^T$. Consequently, the proposed scheme achieves spectral efficiency of $\log_2(M)$ bits per channel use (bpcu) with a half number of LEDs, compared to the GLIM-OFDM.

The average electrical received signal-to-noise ratio (SNR) is given by [12], [13]

$$\gamma = \frac{1}{\sigma_w^2} \xi \left(\frac{1}{P} \sum_{p=1}^P \sum_{l=1}^L h_{p,l} I \right)^2, \quad (3)$$

where ξ denotes the electrical-to-optical conversion factor that is taken as a unity and I represents mean optical intensity that is emitted from LEDs. The M -QAM constellation is assumed to be normalized in order to have unit-energy symbols [13].

The magnitudes and wrap-phases follow the Rayleigh distribution and uniform distribution, respectively. Consequently, the average value of I in (3) can be obtained as

$$I = \frac{\mathbb{E}[x_{k,r}] + \mathbb{E}[x_{k,\theta}]}{2}, \quad (4)$$

where $\mathbb{E}[\cdot]$ denotes the expectation operator. Thus, the average value of I is

$$I = \frac{1}{2} \left[\int_0^\infty x_r^2 \exp\left(-\frac{x_r^2}{2}\right) dx_r + \frac{1}{2\pi} \int_0^{2\pi} x_\theta dx_\theta \right] \\ = \frac{1}{2} \left(\sqrt{\frac{\pi}{2}} + \pi \right). \quad (5)$$

To ensure that the magnitudes and wrap-phases of the OFDM samples stay within the dynamic range of the LEDs, $x_{k,r}$ and $x_{k,\theta}$ are scaled as [7]

$$x_{k,r}^s = s_1 x_{k,r} \quad x_{k,\theta}^s = s_2 x_{k,\theta}, \quad (6)$$

where $x_{k,r}^s$ and $x_{k,\theta}^s$ are the scaled values of $x_{k,r}$ and $x_{k,\theta}$, respectively. Here, s_1 and s_2 are the magnitude and wrap-phase scaling factors, respectively, and expressed as

$$s_1 = \frac{I_{\max} - I_{\min}}{\max\{x_{k,r}\}}, \quad s_2 = \frac{I_{\max} - I_{\min}}{\max\{x_{k,\theta}\}}, \quad (7)$$

where I_{\max} and I_{\min} define the maximum and minimum LED current, respectively. Thus, after normalization, the value of I in (3) becomes

$$I = \frac{1}{2} \left(s_1 \sqrt{\frac{\pi}{2}} + s_2 \pi \right). \quad (8)$$

III. MW-OFDM ESTIMATOR ANALYSIS

In this section, the MLE and BLUE are derived for the proposed MW-OFDM. Moreover, the decoding complexity is analyzed and compared to the GLIM-OFDM schemes.

A. Maximum Likelihood Estimator

Let $\Lambda = [x_{1,r}, \dots, x_{L/2,r}]^T$ define the set of magnitudes of transmitted OFDM samples. Furthermore, let $\Theta = [x_{1,\theta}, \dots, x_{L/2,\theta}]^T$ denote the set of wrap-phases for transmitted OFDM samples. Consequently, (2) can be rewritten as

$$\mathbf{y} = \mathbf{H}_r \Lambda + \mathbf{H}_\theta \Theta + \mathbf{w}, \quad (9)$$

where \mathbf{H}_r and \mathbf{H}_θ are the odd and even columns of \mathbf{H} , respectively. Therefore, the MLE for Λ and Θ can be obtained as

$$\{\hat{\Lambda}, \hat{\Theta}\} = \arg \max_{\Lambda, \Theta} p(\mathbf{y} | \Lambda, \Theta), \quad (10)$$

where $p(\mathbf{y} | \Lambda, \Theta)$ is the probability density function (PDF) of \mathbf{y} , given Λ and Θ , and considering that Λ and Θ are independent. Since the PDF of \mathbf{y} given Λ and Θ is $\mathcal{N}(\mathbf{H}_r \Lambda + \mathbf{H}_\theta \Theta, \sigma_w^2 \mathbf{I})$, and after simple manipulations, the MLE in (10) becomes

$$\{\hat{\Lambda}, \hat{\Theta}\} = \arg \min_{\Lambda, \Theta} \mathcal{M}^{\text{MLE}}(\Lambda, \Theta), \quad (11)$$

where $\mathcal{M}^{\text{ML}}(\Lambda, \Theta)$ is MLE metric that is defined as

$$\mathcal{M}^{\text{MLE}}(\Lambda, \Theta) = \|\mathbf{y} - \mathbf{H}_r \Lambda + \mathbf{H}_\theta \Theta\|^2. \quad (12)$$

Using $\|\mathbf{a}\|^2 = \mathbf{a}^T \mathbf{a}$, (12) becomes

$$\mathcal{M}^{\text{MLE}}(\Lambda, \Theta) = \mathbf{y}^T \mathbf{y} + \Lambda^T \mathbf{H}_r^T \mathbf{H}_r \Lambda + \Theta^T \mathbf{H}_\theta^T \mathbf{H}_\theta \Theta \\ + 2\Lambda^T \mathbf{H}_r^T \mathbf{H}_\theta \Theta - 2\mathbf{y}^T \mathbf{H}_r \Lambda - 2\mathbf{y}^T \mathbf{H}_\theta \Theta. \quad (13)$$

Taking the derivative of $\mathcal{M}^{\text{MLE}}(\Lambda, \Theta)$ in (13) with respect to Λ and Θ and setting the results to zero, the MLE can be formulated as

$$\hat{\mathbf{x}}^{(\text{MLE})} = [\mathbf{A}^{-1} \mathbf{b}]^+, \quad (14)$$

where $[x]^+ := \max([0, x])$ and $\hat{\mathbf{x}} = [\hat{\Lambda} \ \hat{\Theta}]^T$ is the vector of estimated magnitudes and wrap-phases. In (14), \mathbf{A} and \mathbf{b} are calculated as

$$\mathbf{A} = \begin{bmatrix} \mathbf{H}_r^T \mathbf{H}_r & \mathbf{H}_r^T \mathbf{H}_\theta \\ \mathbf{H}_\theta^T \mathbf{H}_r & \mathbf{H}_\theta^T \mathbf{H}_\theta \end{bmatrix}, \quad \mathbf{b} = [\mathbf{H}_r^T \mathbf{y} \quad \mathbf{H}_\theta^T \mathbf{y}]^T. \quad (15)$$

After this point, the estimated magnitudes $\hat{\Lambda}$ and wrap-phases $\hat{\Theta}$ are converted into complex samples as $\hat{\Lambda} \exp(j\hat{\Theta})$. Subsequently, the classical steps of the OFDM, such as the serial-to-parallel (S/P), FFT operations and M -QAM demodulator are used to obtain the estimated information bit-stream.

B. Best Linear Unbiased Estimator

As a low complexity alternative, we also consider the BLUE which does not require the knowledge of a complete PDF. The BLUE can be obtained by using only the knowledge of the mean and covariance of the PDF [15, Ch. 6]. To find the BLUE of $\mathbf{x} := [\Lambda \ \Theta]^T$, the received signal model in (9) should be reformulated in a general linear model as

$$\mathbf{y} = \tilde{\mathbf{H}} \mathbf{x} + \mathbf{w}, \quad (16)$$

where $\tilde{\mathbf{H}} := [\mathbf{H}_r \ \mathbf{H}_\theta]$, $\mathbf{w} \sim \mathcal{N}(\mathbf{0}, \sigma_w^2 \mathbf{I})$, $\mathbf{0} = [0 \ \dots \ 0]^T$ denotes a zero vector and \mathbf{I} represents the identity matrix. Following the Gauss-Markov theorem in [15, Ch. 6] the BLUE of \mathbf{x} can be expressed as

$$\hat{\mathbf{x}}^{(\text{BLUE})} = \left[\left(\tilde{\mathbf{H}}^T (\sigma_w^2 \mathbf{I})^{-1} \tilde{\mathbf{H}} \right)^{-1} \tilde{\mathbf{H}}^T (\sigma_w^2 \mathbf{I})^{-1} \mathbf{y} \right]^+. \quad (17)$$

It is worth noting that the BLUE for a general linear model and Gaussian data is identical to the minimum variance unbiased (MVU) estimator [15, Ch. 6]. On the other hand, the MLE for linear model and Gaussian data attains the MVU estimator [15, Ch. 7]. Consequently, the BLUE in (17) achieves the same BER performance as the MLE in (14). However, the difference between the MLE and BLUE is that the MLE requires the knowledge of the complete PDF while the BLUE requires only the mean and covariance of the PDF.

C. Decoding Complexity

In this subsection, the decoding complexity of the conventional GLIM-OFDM schemes in [12]–[14] is compared to the proposed MW-OFDM scheme. The decoding complexity can be measured by the required number of real additions and real multiplications [13]. In our complexity analysis, the subtraction and division operations are respectively considered as equivalent to addition and multiplication operations.

For the benchmarking 4×4 GLIM-OFDM in [12], [13], the overall real multiplications and additions are respectively calculated as

$$\text{Mul}_{4 \times 4 \text{ GLIM}} = (24P + 68)N, \quad (18)$$

$$\text{Add}_{4 \times 4 \text{ GLIM}} = 24PN. \quad (19)$$

The overall required operations for the 8×8 GLIM-OFDM in [14] are respectively expressed as

$$\text{Mul}_{8 \times 8 \text{ GLIM}} = (656P + 594)N, \quad (20)$$

$$\text{Add}_{8 \times 8 \text{ GLIM}} = (592P + 304)N. \quad (21)$$

For the proposed MW-OFDM, the cost of forming \mathbf{A} and \mathbf{b} in (15) for N OFDM subcarriers requires $P(L^2 + L)N$

real multiplications and $(P-1)(L^2+L)N$ real additions. For solving an $L \times L$ linear system equation utilizing the Gauss elimination, the required operations of real multiplications and additions are $(L^3+3L^2-L)/3$ and $(3L^3+3L^2-5L)/6$, respectively [16]. Consequently, the overall real multiplications and additions for $P \times L$ MW-OFDM in (14) can be respectively given as

$$\text{Mul}_{\text{MW}} = \frac{1}{3}L^3N + (P+1)L^2N + \left(P - \frac{1}{3}\right)LN, \quad (22)$$

$$\text{Add}_{\text{MW}} = \frac{1}{3}L^3N + \left(P - \frac{1}{2}\right)L^2N + \left(P - \frac{11}{6}\right)LN. \quad (23)$$

As a performance metric to demonstrate the saving in the decoding complexity of the proposed MW-OFDM over the existing ones, we define the reduction ratio as

$$\Gamma = \frac{|C_{\Xi} - C_{\text{MW}}|}{C_{\Xi}}\%, \quad (24)$$

where C_{MW} represents the decoding complexity (i.e., multiplications or additions) of the proposed MW-OFDM scheme, and C_{Ξ} denotes the decoding complexity of the compared scheme with $\Xi \in \{4 \times 4 \text{ GLIM-OFDM [12], [13]}, 8 \times 8 \text{ GLIM-OFDM [14]}\}$ using (18)-(23). For example, for $P = 4$ and $L = 2$, the reduction ratio is calculated as $\Gamma = 80\%$ using the proposed MW-OFDM scheme compared to 4×4 GLIM-OFDM in [12], [13]. The reduction ratio becomes $\Gamma = 96\%$ using the proposed scheme with $P = 8$ and $L = 4$ in comparison with 8×8 GLIM-OFDM in [14].

IV. NUMERICAL RESULTS AND DISCUSSIONS

In this section, BER performance comparisons of the proposed MW-OFDM scheme using the MLE given in (14) and conventional GLIM-OFDM schemes using the MAP estimator are provided with respect to the average electrical received SNR given in (3). In addition, the BER performance of the MIMO U-OFDM scheme is included in the comparisons. BER results comparisons versus the average received SNR are presented for different spectral efficiencies (in bpcu) over MIMO VLC channels. The number of the FFT subcarriers is considered as $N = 256$ [13] and the channel state information is assumed to be perfectly known at the receiver side. To ensure a fair comparison, a fixed transmit power is considered for the proposed MW-OFDM and conventional optical MIMO-OFDM schemes. In other words, the average value of the emitted optical intensity I for the proposed scheme and conventional optical MIMO-OFDM schemes are considered to be equal, and $I = 1/2\sqrt{\pi}$. Consequently, the values of s_1 and s_2 are chosen to be $1/\sqrt{2\pi}$ and $1/2\pi^{3/2}$, respectively. The VLC channel matrices for two scenarios of 4×4 MIMO setups and one scenario of a 8×8 MIMO setup are given as [5], [13]

$$\mathbf{H}_1 = 10^{-5} \times \begin{pmatrix} 0.3489 & 0.3288 & 0.3104 & 0.3288 \\ 0.3288 & 0.3489 & 0.3288 & 0.3104 \\ 0.3104 & 0.3288 & 0.3489 & 0.3288 \\ 0.3288 & 0.3104 & 0.3288 & 0.3489 \end{pmatrix}, \quad (25)$$

$$\mathbf{H}_2 = 10^{-6} \times \begin{pmatrix} 0.5356 & 0.6831 & 0.3838 & 0.5762 \\ 0.3354 & 0.3440 & 0.5461 & 0.5121 \\ 0.3414 & 0.3161 & 0.5987 & 0.6031 \\ 0.6958 & 0.5614 & 0.4428 & 0.2052 \end{pmatrix}, \quad (26)$$

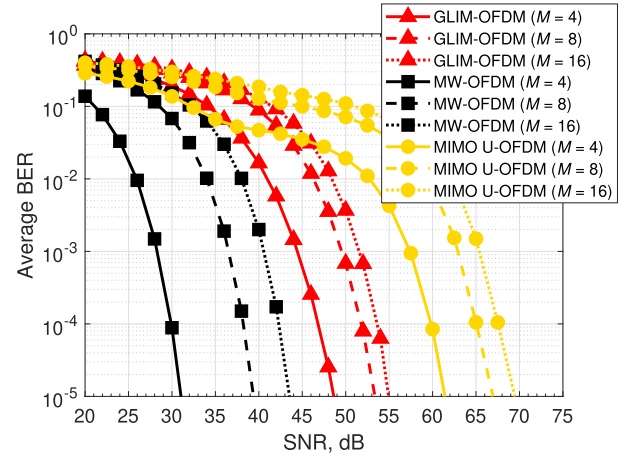


Fig. 2. BER performance of the proposed MW-OFDM and conventional optical MIMO-OFDM schemes for 2 (straight), 3 (dashed) and 4 (dotted) bpcu over channel \mathbf{H}_1 .

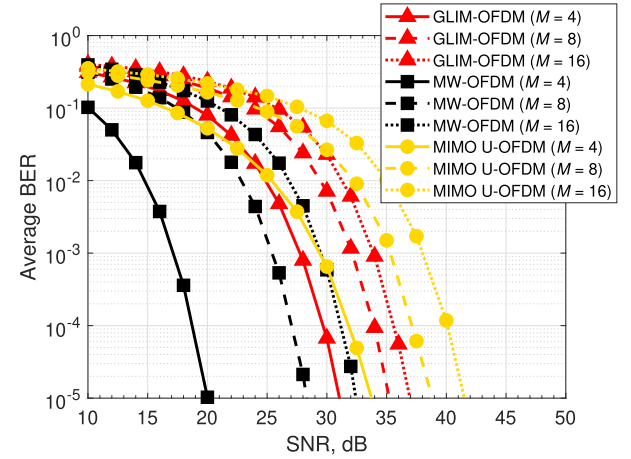


Fig. 3. BER performance of the proposed MW-OFDM and conventional optical MIMO-OFDM schemes for 2 (straight), 3 (dashed) and 4 (dotted) bpcu over channel \mathbf{H}_2 .

$$\mathbf{H}_3 = 10^{-6} \times \begin{pmatrix} 0.377 & 0.483 & 0.446 & 0.523 & 0.400 & 0.466 & 0.273 & 0.430 \\ 0.455 & 0.407 & 0.395 & 0.427 & 0.384 & 0.362 & 0.304 & 0.141 \\ 0.236 & 0.243 & 0.300 & 0.136 & 0.356 & 0.384 & 0.388 & 0.382 \\ 0.316 & 0.202 & 0.300 & 0.119 & 0.353 & 0.164 & 0.349 & 0.478 \\ 0.211 & 0.206 & 0.270 & 0.266 & 0.327 & 0.362 & 0.428 & 0.426 \\ 0.240 & 0.224 & 0.285 & 0.343 & 0.304 & 0.338 & 0.426 & 0.450 \\ 0.391 & 0.501 & 0.388 & 0.413 & 0.345 & 0.344 & 0.312 & 0.122 \\ 0.490 & 0.397 & 0.401 & 0.389 & 0.350 & 0.338 & 0.315 & 0.153 \end{pmatrix}. \quad (27)$$

Figs. 2 and 3 present the average BER performance of the proposed MW-OFDM with $P = 4$ and $L = 2$, compared to the conventional 4×4 GLIM-OFDM in [12], [13] and 4×4 MIMO U-OFDM for spectral efficiencies of 2, 3 and 4 bpcu. In Fig. 2, the BER results of the schemes are provided over \mathbf{H}_1 given in (25), while Fig. 3 describes the BER curves over \mathbf{H}_2 given in (26).

It is observed from Figs. 2 and 3 that the proposed MW-OFDM can achieve much better BER performance compared to the conventional optical MIMO-OFDM (i.e., GLIM-OFDM and MIMO U-OFDM) schemes. For instance, at the BER of

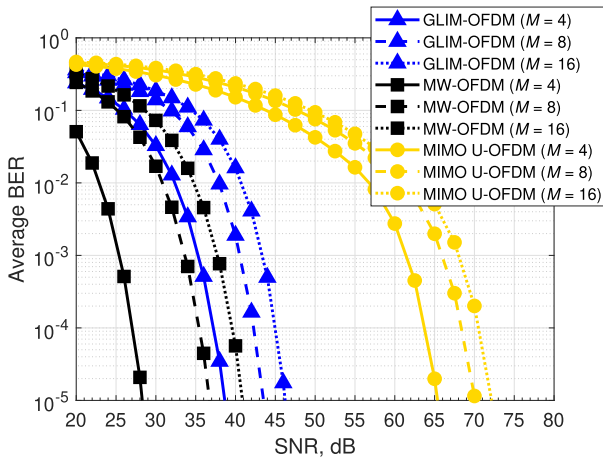


Fig. 4. BER performance of the proposed MW-OFDM and conventional optical MIMO-OFDM schemes for 4 (straight), 6 (dashed) and 8 (dotted) bpcu over channel \mathbf{H}_3 .

10^{-5} in Fig. 2, the required SNR values for the GLIM-OFDM and MIMO U-OFDM schemes are respectively: 48.5 dB and 61.3 dB in order to provide spectral efficiency of 2 bpcu; 53 dB and 67 dB for spectral efficiency of 3 bpcu; 55 dB and 69.4 dB to obtain spectral efficiency of 4 bpcu. Whereas by using the proposed MW-OFDM scheme, the required SNR values to obtain 2, 3 and 4 bpcu are decreased to 31, 39 and 43.5 dB, respectively. This indicates that the proposed scheme can improve the BER performance by 17.5 dB, 14 dB and 11.5 dB for spectral efficiencies of 2, 3 and 4 bpcu, respectively, compared to the GLIM-OFDM. While the proposed scheme enhances the BER performance by 30.3 dB, 28 dB and 25.9 dB in a comparison with the MIMO U-OFDM for these reference bpcu values. In Fig. 3, the proposed scheme enhances the BER performance to provide these three reference bpcu values at the BER of 10^{-5} respectively by 11 dB, 7 dB and 4.5 dB in a comparison with the conventional GLIM-OFDM; and 13.7 dB, 10.5 dB and 9 dB compared to MIMO U-OFDM.

In Fig. 4, we depict the BER performance of the proposed MW-OFDM scheme with $P = 8$ and $L = 4$, compared to the 8×8 GLIM-OFDM in [14] and 8×8 MIMO U-OFDM over \mathbf{H}_3 given in (27). The BER results in Fig. 4 are obtained for the spectral efficiencies of 4, 6 and 8 bpcu, where two samples are simultaneously transmitted using 4-QAM, 8-QAM and 16-QAM, respectively. It can be shown from the results in this figure that the proposed MW-OFDM scheme achieves a better BER performance than both the GLIM-OFDM and MIMO U-OFDM for the same spectral efficiency. For instance, the proposed scheme improves the BER performance by 11, 7 and 6 dB for the spectral efficiencies of 4, 6 and 8 bpcu, respectively, compared to the GLIM-OFDM scheme. Whereas the proposed scheme significantly enhances the BER performance in comparison to the MIMO U-OFDM.

It can be observed from these results that the proposed scheme significantly outperforms the conventional optical MIMO-OFDM schemes for different spectral efficiencies and over different MIMO VLC channels scenarios. Furthermore, the proposed scheme offers a significant reduction in the

decoding complexity at a required half number of LEDs compare to the existing GLIM-OFDM schemes as indicated in Section III-C.

V. CONCLUSION

In this letter, a novel MW-OFDM scheme has been proposed to overcome the restriction on the number of LEDs and enhance the average BER performance in a comparison with existing GLIM-OFDM schemes. The proposed MW-OFDM transmits the magnitudes and wrap-phases of the complex OFDM samples, while a low complexity MLE and BLUE have been derived. At the same spectral efficiency, the proposed MW-OFDM scheme can achieve a BER performance improvement up to 17.5 dB and reduce the decoding complexity up to 96%, while requiring only a half number of LEDs in a comparison with the existing GLIM-OFDM schemes.

REFERENCES

- [1] Z. Ghassemlooy, L. N. Alves, S. Zvanovec, and M.-A. Khalighi, *Visible Light Communications: Theory and Applications*. Boca Raton, FL, USA: CRC Press, 2017.
- [2] M. Uysal, C. Capsoni, Z. Ghassemlooy, A. Boucouvalas, and E. Udvarý, *Optical Wireless Communications: An Emerging Technology*. Cham, Switzerland: Springer, 2016.
- [3] Z. Wang, Q. Wang, W. Huang, and Z. Xu, *Visible Light Communications: Modulation and Signal Processing*. Hoboken, NJ, USA: Wiley, 2017.
- [4] R. Mesleh, H. Elgala, and H. Haas, "On the performance of different OFDM based optical wireless communication systems," *IEEE/OSA J. Opt. Commun. Netw.*, vol. 3, no. 8, pp. 620–628, Aug. 2011.
- [5] M. Al-Nahhal, E. Basar, and M. Uysal, "Adaptive unipolar MIMO-OFDM for visible light communications," in *Proc. Eur. Conf. Netw. Commun. (EuCNC)*, Jun. 2019, pp. 73–77.
- [6] H. Elgala and T. D. C. Little, "P-OFDM: Spectrally efficient unipolar OFDM," in *Proc. Opt. Fiber Commun. Conf.*, 2014, pp. 1–3.
- [7] H. Elgala and T. D. C. Little, "Polar-based OFDM and SC-FDE links toward energy-efficient Gbps transmission under IM-DD optical system constraints [invited]," *J. Opt. Commun. Netw.*, vol. 7, no. 2, p. A277, Feb. 2015.
- [8] S. Guo, K.-H. Park, and M.-S. Alouini, "Adaptive power allocation for distortion minimization in generalized polar optical wireless communications," *IEEE Trans. Commun.*, vol. 67, no. 12, pp. 8545–8556, Dec. 2019.
- [9] T. Lakshmi Narasimhan, R. Tejaswi, and A. Chockalingam, "Quad-LED and dual-LED complex modulation for visible light communication," 2015, *arXiv:1510.08805*. [Online]. Available: <http://arxiv.org/abs/1510.08805>
- [10] A. K. Gupta and A. Chockalingam, "Performance of MIMO modulation schemes with imaging receivers in visible light communication," *J. Lightw. Technol.*, vol. 36, no. 10, pp. 1912–1927, May 15, 2018.
- [11] K. V. S. S. Sushanth and A. Chockalingam, "Multiple-LED complex modulation schemes for indoor MIMO VLC systems," in *Proc. IEEE Int. Conf. Commun. (ICC)*, May 2019, pp. 1–6.
- [12] E. Basar, E. Panayirci, M. Uysal, and H. Haas, "Generalized LED index modulation optical OFDM for MIMO visible light communications systems," in *Proc. IEEE Int. Conf. Commun. (ICC)*, May 2016, pp. 1–5.
- [13] A. Yesilkaya, E. Basar, F. Miramirkhani, E. Panayirci, M. Uysal, and H. Haas, "Optical MIMO-OFDM with generalized LED index modulation," *IEEE Trans. Commun.*, vol. 65, no. 8, pp. 3429–3441, Aug. 2017.
- [14] M. Le Tran, S. Kim, T. Ketseoglou, and E. Ayanoglu, "LED selection and MAP detection for generalized LED index modulation," *IEEE Photon. Technol. Lett.*, vol. 30, no. 19, pp. 1695–1698, Oct. 1, 2018.
- [15] S. M. Kay, *Fundamentals of Statistical Signal Processing: Estimation Theory*. Upper Saddle River, NJ, USA: Prentice-Hall, 1993.
- [16] I. Al-Nahhal, O. A. Dobre, E. Basar, C. Moloney, and S. Ikki, "A fast, accurate, and separable method for fitting a Gaussian function [tips & tricks]," *IEEE Signal Process. Mag.*, vol. 36, no. 6, pp. 157–163, Nov. 2019.